

Sintering Inhibition Mechanism of Platinum on Ceria-based Oxide Support for Automotive Catalysts

Yasutaka Nagai, Kazuhiko Dohmae, Hirofumi Shinjo, Takeshi Hirabayashi,
Nobuyuki Takagi, Takashi Minami, Shinichi Matsumoto

Abstract

The sintering of precious metal particles during the operation of automotive three-way catalysts is considered to reduce the catalytic activity, that is, degrade the catalyst. In this paper, we demonstrated that the Pt particles in Pt/ceria-based catalysts did not sinter at all during high-temperature ageing in an oxidizing atmosphere, in contrast with conventional Pt/Al₂O₃ catalysts.

The sintering inhibition mechanism of Pt in Pt/ceria-based oxide catalyst has been studied using X-ray absorption spectroscopy. We found that the Pt-O-Ce bond, which is the Pt-oxide-support interaction, functioned as an anchor and inhibited the sintering of Pt particles on ceria-based oxide.

Keywords

Platinum, Sintering, Pt-oxide-support interaction, XAFS, Automotive catalyst

1. Introduction

Three-way catalysts (TWCs) can efficiently purify harmful automobile emissions. Since being commercialized in the USA and Japan in 1977,¹⁾ TWCs have played an important role in environmental protection. Recently, due to increasing demands for global environmental protection, more stringent regulations have been imposed on the automobile industry. As a result, automobile companies are striving to purify automobile exhaust emissions. Consequently, there is a strong demand to produce more advanced TWCs by technical innovation.

Three-way catalysts are composed of three components, namely, a precious metal such as Pt or Rh, a support such as Al₂O₃, and an oxygen storage component which is generally a ceria-based oxide.²⁻⁴⁾ The precious metal particles are a few nanometers in diameter and are dispersed on a support oxide. These precious metals function as active sites that extract harmful components from automotive exhausts, such as nitrogen oxides (NO_x), carbon monoxide (CO) and unburned hydrocarbons (HC). When a TWC is exposed to a high temperature of about 800 °C or greater, the precious metal will agglomerate and sinter, reducing the active surface area of the catalyst.⁵⁻⁸⁾ Generally, sintering of the precious metal particles during operation is considered to reduce the catalytic activity, that is, degrade the catalyst. In addition, the exhaust from an automotive gasoline engine fluctuates between an oxidizing and a reducing atmosphere during vehicle operation. Specifically, the activity of Pt-supported catalysts decreases considerably more due to sintering of the Pt particles during high-temperature ageing in an oxidizing atmosphere than in a reducing atmosphere.^{5,6)} Thus, the development of highly durable catalysts that do not undergo Pt sintering in an oxidizing atmosphere is a current goal of automotive industrial research.

Ceria-based oxides are widely utilized in automotive catalysts because they not only store/release oxygen, but they also stabilize precious metal dispersion.^{2, 9)} Several studies have investigated Pt sintering and Pt-support interaction in Pt/ceria catalysts and significant progress has

been made. Diwell et al.¹⁰⁾ reported that the formation of Pt-ceria complexes under oxidizing conditions could prevent Pt from sintering. In addition, Murrell et al.¹¹⁾ showed by using a Laser Raman technique that the precious metal oxide structure interacts strongly with the ceria surface. However, the nature of the Pt-ceria interaction is very complicated and is still not fully understood. Thus, there is room for further investigation of this phenomenon.

In this paper, we investigated the sintering inhibition mechanism of Pt particles on a ceria-based oxide at the atomic level using X-ray absorption spectroscopy.¹²⁾

2. Experimental

2.1 Catalyst preparation and ageing treatment

Pt/Al₂O₃ and Pt/ceria-based mixed oxide (Ce-Zr-Y mixed oxide, referred to as CZY) catalysts were prepared by the following methods. Al₂O₃ and CZY powders were used as support oxides Al₂O₃ was supplied by Nikki Universal Co., Ltd. and it had a γ -type crystal structure. Ce-Zr-Y mixed oxide powders were prepared using a coprecipitation process with aqueous NH₃ using Ce(NO₃)₃, ZrO(NO₃)₂ and Y(NO₃)₃ in aqueous solutions. The precipitate was dried at 110 °C and calcined in air at 700 °C for 3 h. It contained 50 wt% CeO₂, 46 wt% ZrO₂ and 4 wt% Y₂O₃, and its crystal structure was cubic. 2 wt% Pt/Al₂O₃ and 2 wt% Pt/CZY catalysts were prepared by conventional wet impregnation of Al₂O₃ and CZY powders with Pt(NH₃)₂(NO₂)₂ aqueous solution. The impregnated powders were dried overnight at 110 °C and calcined at 500 °C for 3 h in air. These samples are referred to hereafter as the "fresh catalyst". A portion of the fresh sample was aged in air for 5 h at 800 °C. This ageing treatment corresponds to an accelerated test for durability in an oxidizing atmosphere. These samples are referred to hereafter as the "aged catalyst".

The aged Pt/CZY was reduced using 5 % H₂ (N₂ balance) at 400 °C for 30 min. The reduced sample was cooled to room temperature, and then stored in a bag containing an oxygen scavenger to prevent oxidation. The fresh and aged samples were put into a bag that did not contain an oxygen scavenger.

These samples were used in the X-ray absorption fine structure (XAFS) experiment.

2. 2 Characterization

2. 2. 1 Adsorption methods

The specific surface areas of the samples were estimated using the N₂ adsorption isotherm at -196 °C by the one-point Brunauer-Emmett-Teller method employing an automatic surface analyzer (Micro Sorp 4232II, Micro Data Co., Ltd.). The samples were pretreated in flowing N₂ at 200 °C for 20 min. The Brunauer-Emmett-Teller surface areas of the fresh and aged catalysts examined in this study are summarized in **Table 1**, together with the specifications of the supports.

The average particle size of the Pt metal was measured using a CO pulse adsorption method.¹³⁾ The catalysts were pre-treated in flowing pure oxygen, and then pure hydrogen at 400 °C. With this reducing treatment of hydrogen, Pt is reduced to Pt metal. CO pulse adsorption was carried out in flowing He at -78 °C. At this temperature, the CO uptake of the ceria support was almost entirely suppressed, and CO was adsorbed on only the Pt surface.¹⁴⁾ The average particle size was calculated from the CO uptake by assuming that CO was adsorbed on the surface of spherical Pt particles at a stoichiometry of CO/(surface Pt atom) = 1/1.

2. 2. 2 Structure analysis

The microstructure of the catalysts was investigated by transmission electron microscopy (TEM) using a JEOL JEM-2000EX.

The powder X-ray diffraction (XRD) experiments

were performed in air at room temperature using a RINT2000 (Rigaku Co. Ltd.) diffractometer with Cu K α radiation (wavelength: 1.5406 Å). The catalyst samples were reduced by 5 % H₂ (N₂ balance) at 400 °C for 30 min before performing the XRD measurement. The catalyst powder was pressed into wafers and attached to standard-sized microscope slides. The average particle size of Pt was estimated from the Pt(1 1 1) line width using Scherrer's equation with the Gaussian line shape approximation.

The Pt L₃-edge (11.5 keV) XAFS measurement was carried out at BL01B1 and BL16B2 of SPring-8 (Hyogo, Japan). The storage ring energy was 8 GeV with a typical current of 100 mA. The XAFS spectra at the Pt L₃-edge were measured using a Si (1 1 1) double-crystal monochromator in fluorescence mode at room temperature in air. Data reduction of the XAFS spectra was carried out as described elsewhere.¹⁵⁾ Curve-fitting analysis of the extended X-ray absorption fine structure (EXAFS) spectra was performed on the inverse Fourier transforms for the Pt-O and Pt-cation (where cation = Pt, Ce and Zr) shells using the theoretical parameters calculated by McKale et al.¹⁶⁾

The X-ray photoelectron spectroscopy (XPS) measurements were carried out using a PHI model 5500MC with Mg K α X-rays. The catalyst sample was placed on a grid and pretreated under 0.5 atm O₂ pressure at 500 °C for 5 min. The pretreated sample was cooled to room temperature and then transferred to the XPS measurement stage without being exposure to air. The oxygen 1s core electron levels in the support oxides were recorded to evaluate the chemical properties of the support. The binding energies were calibrated with respect to Pt(4f_{7/2}) at 71.4 eV.

3. Results and discussion

3. 1 Sintering of Pt particles in Pt/Al₂O₃ and Pt/CZY catalysts

First of all, the Pt sintering behaviors of the Pt/Al₂O₃ and Pt/CZY catalysts were investigated. **Figure 1** shows TEM images of the Pt/Al₂O₃ and Pt/CZY catalysts after ageing treatment at 800 °C in air for 5 h. Large Pt particles ranging in size from 3 to 150 nm were observed in the aged Pt/Al₂O₃. By

Table 1 The catalyst samples and BET surface area.

Sample ^a	Pt loading (wt %)	Support	BET surface area(m ² /g)	
			Fresh catalyst	Aged catalyst ^b
Pt/Al ₂ O ₃	2	γ -Al ₂ O ₃	185	154
Pt/CZY	2	Ce-Zr-Y mixed oxide, Cubic-type, 50 wt% CeO ₂ -46 wt% ZrO ₂ -4 wt% Y ₂ O ₃	99	58
Pt/CeO ₂	2	Cubic-type CeO ₂	107	81
Pt/SiO ₂	2	Amorphous SiO ₂	51	47
Pt/ZrO ₂	2	Tetragonal + monoclinic-type ZrO ₂	87	30
Pt/TiO ₂	2	Rutile-type TiO ₂	67	34

^a For sample description, see Experimental section.

^b Fresh samples were aged in air for 5 h at 800 °C.

contrast, no Pt particles were observed in the aged Pt/CZY; Pt could only be detected by energy dispersive X-ray analysis. This indicates that the Pt particles are highly dispersed in the CZY support.

The average sizes of the Pt particles for these catalysts were determined using both XRD and the CO pulse method (Table 2). The diffraction peaks from the Pt particles in both fresh Pt/Al₂O₃ and fresh Pt/CZY could not be detected by XRD due to their small particle size. The Pt particle size on the Al₂O₃ support before the ageing treatment, which was estimated by the CO pulse method, was almost the same as that for the fresh CZY, being about 1 nm. This situation changed completely after ageing. The Pt particles in the Pt/Al₂O₃ increased in size during the ageing treatment. The Pt particle sizes in the aged Pt/Al₂O₃ determined by the XRD and CO pulse methods were 61 and 23.6 nm, respectively. On the other hand, Pt particles in the Pt/CZY could not be observed by XRD even after ageing, suggesting that the Pt particles on the CZY support continued to be highly dispersed. The Pt particle size of 1.1 nm in

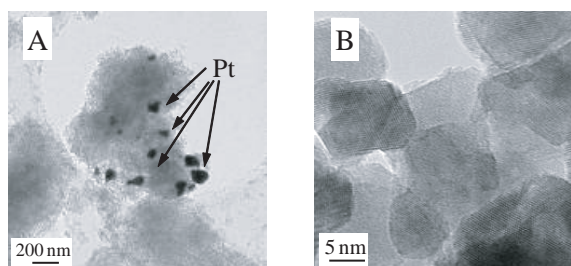


Fig. 1 TEM images of Pt supported catalysts after 800 °C ageing in air for 5 h. (A) Pt/Al₂O₃ catalyst. (B) Pt/CZY catalyst.

Table 2 Average platinum particle size of the catalysts estimated by XRD and CO pulse adsorption method.

Sample		Average Pt particle size (nm)	
		XRD ^a	CO pulse
Pt/Al ₂ O ₃	Fresh	ND ^b	1.0
	Aged	61	23.6
Pt/CZY	Fresh	ND ^b	1.1
	Aged	ND ^b	1.1

^a Average particle size was estimated from Pt(1 1 1) line width.

^b The diffraction peak from the Pt particles could not be detected.

the aged Pt/CZY estimated by the CO pulse method was the same as that in the fresh catalyst. This indicates that Pt in the Pt/CZY catalyst did not sinter at all during the ageing treatment.

3. 2 XAFS analysis of Pt/Al₂O₃ and Pt/CZY catalysts after ageing

In order to clarify the cause of the sintering inhibition of Pt in Pt/CZY, the state of the Pt atoms supported on Al₂O₃ or CZY was investigated using XAFS analysis. Generally, XAFS spectra can be subdivided into two spectral regions, namely the X-ray absorption near edge structure (XANES) and the EXAFS regions. We can obtain information on the electronic state from XANES analysis¹⁷⁾ and on the local structure around a target element from EXAFS analysis.¹⁸⁾

3. 2. 1 Pt L₃-edge XANES spectra

Figure 2 shows the XANES spectra at Pt L₃-edge for the aged catalysts and the reference samples. The steeply rising absorption edge is referred to as the "white line". In the case of the Pt L₃-edge XANES, the absorption intensity of the white line reflects the vacancy in the 5d orbital of Pt atoms.¹⁵⁾ A large white line is observed in oxidized Pt, while a small white line is observed in reduced Pt. Therefore, it is possible to estimate the average oxidation state of the Pt atoms in each sample. The white line intensity of Pt/Al₂O₃ is the same as that of Pt foil. This suggests that Pt on Al₂O₃ is in the Pt⁰ (metal) state after ageing. By contrast, the white line intensity of Pt/CZY is similar to that of PtO₂, suggesting that the Pt²⁺ and Pt⁴⁺ species that have a high oxidation state are mainly present in the aged

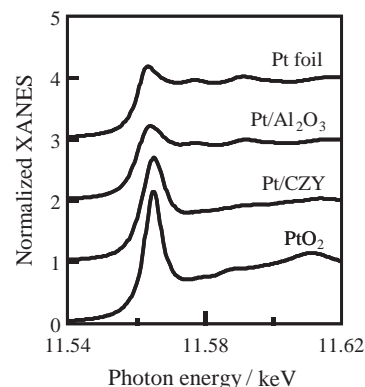


Fig. 2 Pt L₃-edge XANES spectra for supported Pt catalysts after 800 °C ageing in air, together with standard samples of Pt foil and PtO₂ powder.

Pt/CZY. The average oxidation state of Pt can be quantitatively evaluated from the white line intensity.¹⁹⁾ There is a linear relationship between the white line intensity and the oxidation state of PtOx on some metal oxide supports. On the basis of this linear relationship, the estimated oxidation states of Pt in the aged Pt/Al₂O₃ and the aged Pt/CZY were 0 and 3.53, respectively.

Generally, it is well known that PtO₂ decomposes to Pt metal under oxidizing conditions at around 600 °C or above according to the thermodynamic phase diagram.²⁰⁾ The finding that Pt on Al₂O₃ was in the Pt⁰ state after ageing at 800 °C in an oxidizing atmosphere is consistent with thermodynamics. On the other hand, the CZY support could stabilize a high-oxidation state of Pt even after ageing. Thus, it is suggested that the strong Pt-support interaction in the Pt/CZY under the oxidizing condition causes the stabilization of high-oxidation state of Pt.

3. 2. 2 Fourier transforms (FTs) of Pt L₃-edge EXAFS spectra

Fourier transforms (FTs) of the aged catalysts and reference samples are presented in **Fig. 3**. The FTs were performed on the Pt L₃-edge EXAFS spectra in about the 3.0-16 Å⁻¹ region. Quantitative curve-fitting analysis of the EXAFS spectra was performed on the inverse FTs for the Pt-oxygen and Pt-cation (cation = Pt, Ce and Zr) shells, respectively. The results of the curve-fitting analysis are summarized in **Table 3**. In the FT spectrum of Pt foil, the peak at

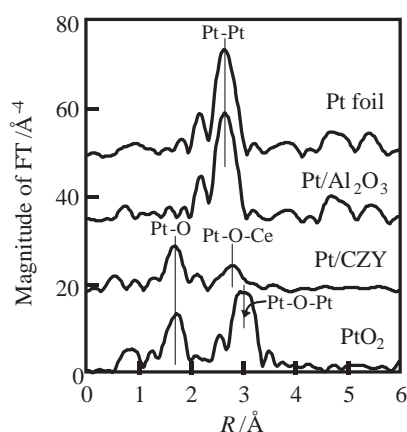


Fig. 3 Fourier-transformed $k^3\chi$ data of Pt L₃-edge EXAFS for supported Pt catalysts after 800 °C ageing in air and the standard samples of Pt foil and PtO₂ powder.

2.76 Å assigned to the Pt-Pt bond. In the FT spectra of the PtO₂ powder, the peaks at 2.04 and 3.10 Å are assigned to the Pt-O and Pt-O-Pt bonds, respectively. The FT spectrum of Pt/Al₂O₃ after ageing is obviously different from that of Pt/CZY. As for the aged Pt/Al₂O₃, only the intense peak at 2.76 Å, which corresponds to the Pt-Pt bond, was observed. The FT spectrum of Pt/Al₂O₃ was similar to that of Pt foil. The coordination number of the Pt-Pt shell in the aged Pt/Al₂O₃ was 11.5. This indicates that the Pt metal particles on Al₂O₃ after ageing are at least 20 nm in size.²¹⁾ The FT spectrum of Pt/CZY after ageing was different from the spectra of both Pt foil and PtO₂ powder. The position of the first peak at 2.02 Å in the Pt/CZY was close to that of PtO₂, and this peak was fitted with the Pt-O bond. It should be noted that the second peak in the spectrum, which was absent in the spectra of both Pt foil and PtO₂ powder, was at 3.01 Å. A curve-fitting simulation of this second peak was carefully performed. **Figure 4** shows the results of curve-fitting analysis on the second peak of the Pt/CZY on the supposition that the second neighboring atom is either Ce or Pt. An excellent fitting result for the simulation of the Ce atom could be obtained. On the other hand, an appropriate fit could not be obtained in the case of Pt, because the EXAFS oscillation pattern of Pt was very different from that of the experimental data. It is clear from this that the second neighboring atom in the aged Pt/CZY is Ce and not Pt. Curve-fitting analysis for other cations such as Zr and Y was also conducted in order to investigate the second neighboring atom in the aged Pt/CZY, but it was not possible to obtain an

Table 3 Results of curve-fitting analysis for the aged catalysts and standard samples.

Sample	Shell	CN	R (Å)	σ ² (Å ²)
Pt foil ^a	Pt-Pt	12.0	2.76	0.0045
Pt/Al ₂ O ₃	Pt-Pt	11.5	2.76	0.0046
Pt/CZY	Pt-O	4.1	2.02	0.0007
	Pt-Ce	3.5	3.01	0.0037
PtO ₂ ^a	Pt-O	5.7	2.04	0.0026
	Pt-Pt	5.3	3.10	0.0019

^a The curve-fitting analyses for the standard samples were performed using the data given in Refs. 22 and 23.

appropriate fit for Ce when compared to Zr(Y). These results lead to the conclusion that Pt atoms strongly interact with the CZY support during ageing and form Pt-O-Ce bonds. The value of the coordination number of the Pt-Ce shell in the aged Pt/CZY was 3.5. This is lower than 12, which is the saturated coordination number for the cubic fluorite structure. This indicates that Pt ions exist on the surface of CZY support. In addition, intense Pt-Pt or Pt-O-Pt peaks could not be observed in the aged Pt/CZY, suggesting that there are no large Pt metal or Pt oxide particles on CZY. In other words, highly dispersed Pt oxides are present on the surface of CZY support.

A similar Pt-O surface complex on CeO₂ has been

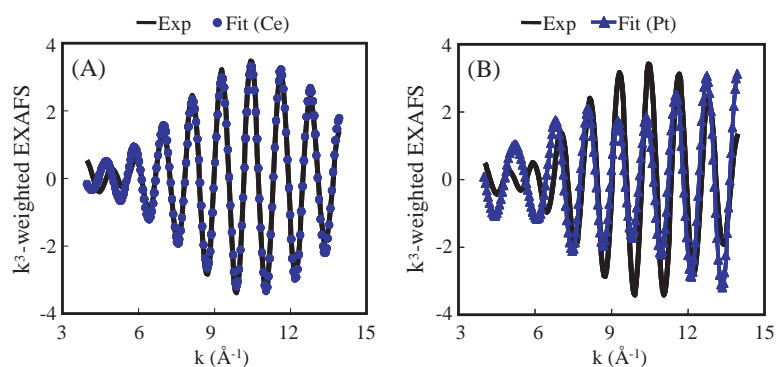


Fig. 4 The results of curve-fitting analysis on the inverse Fourier-transform of the second peak on the aged Pt/CZY catalyst in Fig. 3 and the corresponding curve-fit. (A) Experimental (—) and curve-fit for Ce atom (●). (B) Experimental (—) and curve-fit for Pt atom (▲).

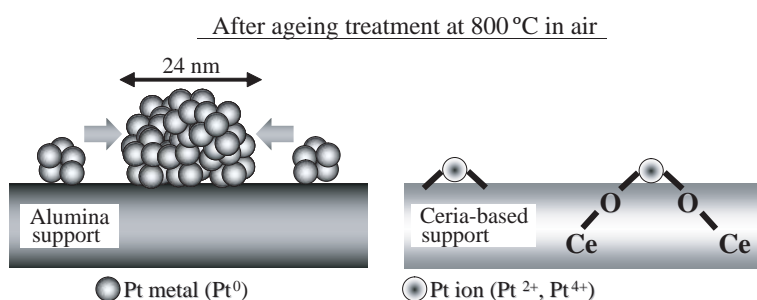


Fig. 5 Schematic illustration of the Pt sintering inhibition mechanism for a Pt/ceria-based catalyst and a conventional Pt/Al₂O₃ catalyst. Since the Pt-Al₂O₃ interaction is weak, Pt metal particles are formed and sintered during 800 °C ageing treatment in air. By contrast, Pt supported on CZY has a strong interaction with CZY support. The generation of a Pt-O-Ce bond prevents Pt particles from sintering during the ageing treatment.

reported by Murrell et al.¹¹⁾ Murrell et al. reported the following, "using laser Raman spectroscopy, a strong Raman band at ca. 700 cm⁻¹ was observed for Rh, Ir, Pd, and Pt dispersed on CeO₂. This Raman band was assigned to a surface oxide metal-O formed on the CeO₂ surface. Metal oxides on CeO₂ exhibit a strong oxide-support interaction." The results of our XAFS analysis could provide direct evidence for the formation of Pt-O-Ce bond on the surface of ceria-based oxide support. Moreover, we showed that this Pt-oxide support interaction on the CZY surface is stronger than that on the Al₂O₃ surface.

3.3 Pt sintering inhibition mechanism

Based on the above observation, we propose the sintering inhibition mechanism of Pt supported on CZY shown in **Fig. 5**. In the case of Pt/Al₂O₃, since the interaction between Pt and Al₂O₃ is weak, Pt particles migrate across the surface of the Al₂O₃ support and sinter during 800 °C ageing treatment in an oxidizing atmosphere according to the molecular migration model.^{6, 24, 25)} By contrast, Pt supported on CZY has a strong interaction with the CZY support. Therefore the CZY support stabilizes the high-oxidation state of Pt, and the formation of a rigid Pt-O-Ce bond acts as an anchor. The formation of Pt-O-Ce bonds on CZY suppresses the sintering of Pt. It is considered that the highly dispersed Pt oxide on the surface of CZY support under oxidizing conditions is more stable since the Pt-O-Ce bond energies are greater than the Pt-Pt bond energies in large Pt crystallites.

It is well known that the sintering of the supported metal occurs not only via the foregoing metal migration, but also by a reduction in the support surface area during ageing treatment.^{6, 24, 25)} The surface areas of the fresh and aged Pt/Al₂O₃ were 185 and 154 m²/g, respectively (Table 1). By contrast, the surface area of Pt/CZY decreased from 99 to 58 m²/g, as shown in Table 1. The

ageing treatment resulted in a 40 % reduction in the surface area of Pt/CZY, compared with only a 17 % reduction in Pt/Al₂O₃. Although the Al₂O₃ support has a high thermal stability when compared to the CZY support, the Pt particles on the Al₂O₃ support sintered significantly. Therefore, the Pt sintering was mainly caused by Pt migration, not by reductions in the surface area of supports. As for the sintering inhibition mechanism, the Pt-O-Ce bond, that is, the Pt-oxide-support interaction inhibits Pt migration, and this is the main reason why Pt supported on CZY does not sinter during the high-temperature ageing in an oxidizing atmosphere.

4. Conclusion

First, based on TEM, XRD and CO-pulse measurements, this study found that Pt supported on ceria-based oxide (CZY) does not sinter under oxidizing conditions at 800 °C while Pt on Al₂O₃ sinters significantly. Pt metal particles on Pt/Al₂O₃ increased in size to 23.6 nm (as measured by the CO-pulse method) during the ageing treatment. On the other hand, Pt metal particles on Pt/CZY after the ageing continued to be highly dispersed having a diameter of about 1 nm.

Second, we clarified the sintering inhibition mechanism of Pt particles on CZY at an atomic level using XAFS analysis. It was found that Pt supported on CZY had a strong interaction with the CZY support. Therefore, the CZY support stabilizes the high-oxidation state of Pt under oxidizing conditions at high temperatures, and strong Pt-O-Ce bonds form as a result of the Pt-oxide-support interaction. The Pt-O-Ce bond acts as an anchor and inhibits Pt migration.

Using advanced analysis techniques such as synchrotron radiation analysis, it is possible to design catalysts for practical use, rather than adopting a trial-and-error approach. We hope that our report can pave the way for planned catalytic design in the future. This approach of designing catalysts at the atomic level by using advanced synchrotron radiation analysis should enable the realization of an ultimate clean car which completely removes harmful components from its exhaust gases in the future.

Acknowledgements

The X-ray absorption experiments were performed at the SPring-8 with the approval of the Japan Synchrotron Radiation Research Institute (JASRI). The authors thank Drs. Uruga and Tanida at SPring-8 for the X-ray measurements.

References

- 1) Matsumoto, S. : "Recent Advances in Automobile Exhaust Catalysts", *Catal. Today*, **90**-3/4(2004), 183
- 2) Yao, H. C. and Yao, Y. F. : "Ceria in Automotive Exhaust Catalysts : 1. Oxygen Storage", *J. Catal.*, **86**-2(1984), 254
- 3) Ozawa, M., Kimura, M. and Isogai, A. : "The Application of Ce-Zr Oxide Solid-Solution to Oxygen Storage Promoters in Automotive Catalysts", *J. Alloys Comp.*, **193**-1/2(1993), 73
- 4) Nagai, Y., Yamamoto, T., Tanaka, T., Yoshida, S., Nonaka, T., Okamoto, T., Suda, A. and Sugiura, M. : "X-ray Absorption Fine Structure Analysis of Local Structure of CeO₂-ZrO₂ Mixed Oxides with the Same Composition Ratio (Ce/Zr=1)", *Catal. Today*, **74**-3/4 (2002), 225
- 5) Harris, P. J. F. : "The Sintering of Platinum Particles in an Alumina-supported Catalyst - Further Transition Electron-Microscopy Studies", *J. Catal.*, **97**-2(1986), 527
- 6) Fiedorow, R. M. J., Chahar, B. S. and Wanke, S. E. : "The Sintering of Supported Metal Catalysts : II. Comparison of Sintering Rates of Supported Pt, Ir, and Rh Catalysts in Hydrogen and Oxygen", *J. Catal.*, **51**-2(1978), 193
- 7) Bartholomew, C. H. : "Mechanisms of Catalyst Deactivation", *Appl. Catal. A*, **212**-1/2(2001), 17
- 8) Birgersson, H., Eriksson, L., Boutonnet, M. and Jaras, S. G. : "Thermal Gas Treatment to Regenerate Spent Automotive Three-way Exhaust Gas Catalysts (TWC)", *Appl. Catal. B*, **54**-3(2004), 193
- 9) Su, E. C. and Rothschild, W. G. : "Dynamic Behavior of Three-way Catalysts", *J. Catal.*, **99**-2(1986), 506
- 10) Diwell, A. F., Rajaram, R. R., Shaw, H. A. and Truex, T. J. : "The Role of Ceria in Three-way Catalysts", *Stud. Surf. Sci. Catal.*, **71**(1991), 139
- 11) Murrell, L. L., Tauster, S. J. and Anderson, D. R. : "Laser Raman Characterization of Surface Phase Precious Metal Oxides Formed on CeO₂", *Stud. Surf. Sci. Catal.*, **71**(1991), 275
- 12) Nagai, Y., Hirabayashi, T., Dohmae, K., Takagi, N., Minami, T., Shinjoh, H. and Matsumoto, S. : "Sintering Inhibition Mechanism of Platinum Supported on Ceria-based Oxide and Pt-oxide-support Interaction", *J. Catal.*, **242**-1(2006), 103
- 13) Uchijima, T. : *Catalytic Science and Technology*, (1990), Kodansha-VCH, Weinheim
- 14) Holmgren, A., Andersson, B. and Duprez, D. : "Interaction of CO with Pt/Ceria Catalysts", *Appl. Catal. B*, **22**-3(1999), 215

- 15) Tanaka, T., Yamashita, H., Tsutitani, R., Funabiki, T. and Yoshida, S. : "X-ray Absorption (EXAFS XANES) Study of Supported Vanadium-oxide Catalysts - Structure of Surface Vanadium-oxide Species on Silica and Gamma-alumina at a Low-level of Vanadium Loading", J. Chem. Soc., Farad. Trans., **84**(1988), 2987
- 16) McKale, A. G., Veal, B. W., Paulikas, A. P., Chan, S. K. and Knapp, G. S. : "Improved Abinitio Calculations of Amplitude and Phase Functions for Extended X-ray Absorption Fine-Structure Spectroscopy", J. Am. Chem. Soc., **110**-12(1988), 3763
- 17) Mansour, A. N., Cook, J. W. and Sayers, D. E. : "Quantitative Technique for the Determination of Unoccupied d-Electron States in a Platinum Catalysts Using the $L_{2,3}$ X-ray Absorption Edge Spectra", J. Phys. Chem. A, **88**(1984), 2330
- 18) Teo, B. K. : EXAFS; Basic Principles and Data Analysis, (1986), Springer, Berlin
- 19) Yoshida, H., Nonoyama, S., Yazawa, Y. and Hattori, T. : "Quantitative Determination of Platinum Oxidation State by XANES Analysis", Physica Scripta, T115(2005), 813
- 20) Livingstone, S. E. : Pergamon Text in Inorganic Chemistry, **25**(1973),
- 21) Greigor, R. B. and Lytle, F. W. : "Morphology of Supported Metal Clusters: Determination by EXAFS and Chemisorption", J. Catal., **63**-2(1980), 476
- 22) Vaarkamp, M. : "Obtaining Reliable Structural Parameters from EXAFS", Catal. Today, **39**-4 (1998), 271
- 23) Lee, A. F., Wilson, K., Lambert, R. M., Hubbard, C. P., Hurley, R. G., McCabe, R. W. and Gandhi, H. S. : "The Origin of SO_2 Promotion of Propane Oxidation over Pt/ Al_2O_3 Catalysts", J. Catal., **184**-2(1999), 491
- 24) Fiedorow, R. M. J. and Wanke, S. E. : "The Sintering of Supported Metal Catalysts : I. Redispersion of Supported Platinum in Oxygen", J. Catal., **43**-1/3 (1976), 34
- 25) Forzatti, P. and Lietti, L. : "Catalyst Deactivation", Catal. Today, **52**-2/3(1999), 165
(Report received on Sept. 14, 2006)


Yasutaka Nagai

Research fields : Automotive catalyst
Academic society : Catalysis Soc. of Jpn.
Awards : 3rd Hyogo Spring-8 Award,
2005


Kazuhiko Dohmae

Research fields : Catalyst analysis
Academic society : Surface Sci. Soc. of
Jpn., Jpn. Soc. for Synchrotron
Radiation Research
Awards : Paper award, Soc. of Automot.
Eng. of Jpn., 2004


Hirofumi Shinjoh

Research fields : Catalysis & catalyst
development
Academic degree : Dr. Eng.
Academic society : Catalysis Soc. of Jpn.,
Chem. Soc. of Jpn., Soc. of Chem.
Eng. of Jpn., Soc. of Automot. Eng.
of Jpn.
Awards : The technology prize , Mech.
Eng. of Jpn., 1995


Takeshi Hirabayashi*

Research fields : Automotive catalyst


Nobuyuki Takagi*

Research fields : Automotive catalyst


Takashi Minami*

Research fields : Materials analysis


Shinichi Matsumoto*

Research fields : Automotive catalyst
Academic degree : Dr. Eng.
Academic society : Catalysis Soc. of Jpn.,
Chem. Soc. of Jpn., Soc. of Chem.
Eng. of Jpn., Soc. of Automot. Eng.
of Jpn.
Awards : The technical development
prize, Soc. of Automot. Eng. of
Jpn., in 1995
The technology prize, Chem. Soc.
of Jpn., 1995
The technology prize, Catalysis
Soc. of Jpn., 2000
The R&D 100 award, 2000

*Toyota Motor Corp.